光学学报

基于电控光学采样的飞秒激光距离测量系统

薛睿，武子铃，董佳琦，胡明列，宋有建*

天津大学精密仪器与光电子工程学院光电信息技术科学教育部重点实验室，天津 300072

摘要　基于电控光学采样原理开展了飞秒激光飞行时间绝对距离测量的实验研究。电控光学采样技术使用两台重复频率锁相的飞秒激光器，分别作为信号激光器和本地振荡器。在本地振荡器的谐振腔内插入电光调制器并施加方波调制，实现了可控、高效的等效时间采样，采样速度由电光调制器的调制频率决定。基于这一采样原理开展脉冲飞行时间绝对距离测量实验。选用一对重复频率约为 158 MHz 的被动锁模光纤激光器作为光源，对固定目标进行单次测量的最大更新速率可达到 200 kHz，经过 4100 次单次测量平均后，测距精度可达到 16.7 nm。在此基础上，测量了硅基微机械器件中深度约为 67.6 μm 的微槽。

关键词　测量；飞秒脉冲；电控光学采样；飞行时间；绝对距离测量

中图分类号　TN249　　**文献标志码**　A　　**DOI**：10.3788/AOS221370

1　引　　言

飞秒激光[1-2]具有脉冲宽度窄、峰值功率高和光谱范围宽等优点，已经成为诸多前沿科学技术和工业领域不可或缺的光源[3-9]。近年来，飞秒激光飞行时间绝对测距技术[10-12]因兼具量程大、精度高、更新速度快和可在线溯源至时间基准等优势，获得了广泛的关注。由于直接光电探测的手段无法提取飞秒精度的脉冲飞行时间，故飞秒激光飞行时间测量通常采用双飞秒激光（或双光梳）[13]的结构。双飞秒激光测量系统利用两台重复频率有微小差异的飞秒激光器作为光源，通过二者在时域上不断地相遇和走离，进行异步光学采样，将探测器无法响应的快变化信号转变为探测器可以响应的慢变化信号。自 2009 年 Coddington 等[14]首次报道以来，基于异步光学采样或飞秒激光绝对距离测量的技术取得了长足的进展[15-20]。

基于异步光学采样的双飞秒激光测距系统的更新速率受制于两台激光器的重复频率差，对于常见的重复频率约为 100 MHz 的激光器而言，其更新速率只能达到几千赫兹。这是因为异步光学采样只能对整个周期进行全部扫描，并进行无差别放大，将大部分的时间都用在了脉冲的相互走离之中。为了打破异步光学采样带来的更新速率的限制，电控光学采样被提出，利用电光调制器控制两个激光脉冲序列的相对延时，从而实现更新速率和扫描范围的调整。电控光学采样已经被应用于太赫兹时域光谱[21-22]、相干光学层析成像[23]和拉曼光谱[24]等领域中，打破了异步光学采样所带来的更新速率的限制，并实现了测量范围的可调谐。

将电控光学采样与飞行时间法相结合进行绝对距离的测量，令其只对信号的回波脉冲进行往返扫描，提升了有效信号的占空比，同时也将更新速率提升了数十倍。2022 年，Shi 等[25]设计并实现了一种基于电控光学采样的双飞秒激光位移测量系统，光源使用了两台重复频率为 105 MHz 的激光器，基于双光子吸收的方式得到测距信号，最高更新速率可达到 80 kHz。本文在此基础上，通过提升激光器的重复频率，以及优化测距光路和解算程序等方式实现了电控光学采样双梳测距系统性能的进一步提升，并且选择利用干涉的方式得到测距信号，相较于双光子吸收的方式，对回光功率的要求更低，有利于对回光较差的物体进行测量。使用两台重复频率皆为 158 MHz 的非线性偏振旋转（NPR）锁模激光器作为光源，利用平衡互相关（BOC）系统[26]进行重复频率的锁定，单次测量的更新速率可以达到 200 kHz，在进行 41 μm 的绝对距离测量时，Allan 方差在平均时间为 20.5 ms 时可以达到 16.7 nm。利用此套系统进行了表面痕迹检测，测量了微机械结构中的凹槽，其深度约为 67.6 μm。

2　实验原理

基于电控光学采样原理实现了飞秒激光飞行时间绝对距离的测量。电控光学采样原理使用了两台重复频率一致的激光器作为光源，其中一台激光器腔内加

收稿日期：2022-06-27；**修回日期**：2022-07-24；**录用日期**：2022-08-03；**网络首发日期**：2022-08-13

基金项目：国家自然科学基金（61827821）、广东省重点领域研发计划（2018B090944001）

通信作者：*yjsong@tju.edu.cn

入电光调制器(EOM),命名为本振激光器,另一台命名为信号激光器。利用腔内 EOM 对本振激光器施加调制,令其输出脉冲在信号激光器输出脉冲的两侧进行走离,从而实现可控且高效的光学采样。

令两台飞秒激光器的输出脉冲进入激光器同步模块中进行同步锁定与对准后,给 EOM 施加一个振幅为 V、频率为 f_m 的方波调制,经过 EOM 中 $LiNbO_3$ 晶体的光就会因线性电光效应产生相位差 $\varphi=\pi V/V_\pi$,其中 V_π 为 EOM 中 $LiNbO_3$ 晶体的半波电压。相位差确定后便可以推导出在 $LiNbO_3$ 晶体中光程的改变量 $\Delta l=\varphi\lambda/(2\pi)=\lambda V/(2V_\pi)$ 和腔长改变量 $\Delta L=\Delta l/n_g=\lambda V/(2V_\pi n_g)$,其中 λ 为本振激光器的中心波长,n_g 为空气的群折射率。

腔长的变化会引起重复频率的改变,将重复频率调制为 $f_r\pm\Delta f_r$ 后,原本对准的两个脉冲会发生走离。脉冲单次走离的距离 ΔL_{mis} 即为腔长改变量 ΔL,相应的表达式为

$$\Delta L_{mis}=\Delta L=\left|\frac{1}{f_r}-\frac{1}{f_r\pm\Delta f_r}\right|\cdot\frac{c}{n_g}\approx\frac{\Delta f_r}{f_r^2}\cdot\frac{c}{n_g},\tag{1}$$

式中:c 为真空中的光速;f_r 为重复频率。由式(1)可推得重复频率变化量 Δf_r 的表达式为

$$\Delta f_r=\frac{\Delta L\cdot f_r^2\cdot n_g}{c}=\frac{\lambda\cdot V\cdot f_r^2}{2V_\pi\cdot c}。\tag{2}$$

将信号发生器产生的频率为 f_m 的方波调制施加给 EOM,其固定调制电压的持续时间为 $1/(2f_m)$。在此持续时间内走离的脉冲数量为 $f_r/(2f_m)$,则累积的走离距离 L_{mis} 可表示为

$$L_{mis}=\Delta L\cdot\frac{f_r}{2f_m}=\frac{\lambda\cdot V\cdot f_r}{4V_\pi\cdot f_m\cdot n_g}。\tag{3}$$

如图 1 所示,本振光在信号光的两侧 L_{mis} 范围内进行往返走离扫描,从而对这一段指定窗口进行放大,得到更新速率为 $2f_m$ 的测距信号,改善了有效信号占空比低的问题,提升了数据的更新速率。

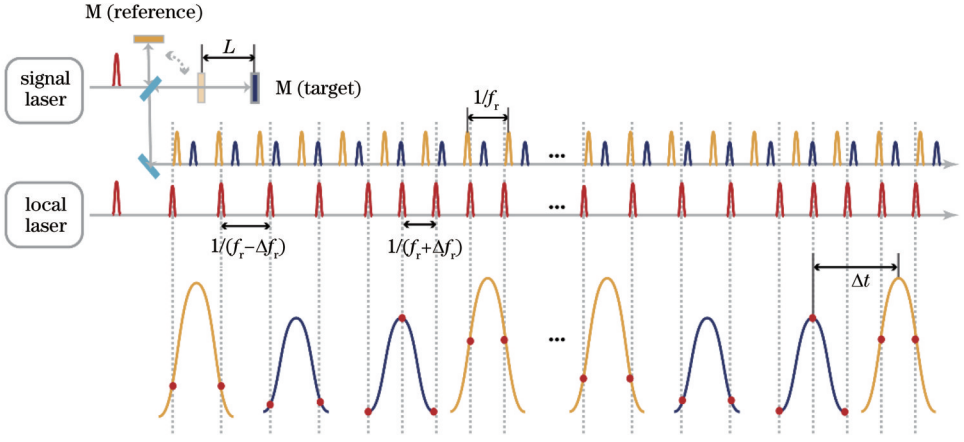

图 1　电控光学采样原理示意图

Fig. 1　Schematic diagram of electronically controlled optical sampling principle

当两个脉冲之间存在脉冲走离时,便可以实现两束光的干涉,实现光学异步采样。在时域上将脉冲放大,将光电探测器无法直接探测到的快变化光脉冲信号转换为光电探测器可以响应的慢变干涉信号,放大倍数为

$$N=\frac{f_r}{\Delta f_r}=\frac{2V_\pi\cdot c}{\lambda\cdot V\cdot f_r}。\tag{4}$$

信号光脉冲被参考镜与目标镜反射后分别可产生参考回波脉冲和目标回波脉冲,通过解算光电探测器探测得到的参考回波脉冲和目标回波脉冲的包络峰值位置,可以解算出二者的时间间隔 Δt,进而可以解算出参考镜与目标镜之间的绝对距离 L,其表达式为

$$L=\frac{c}{2n_g}\cdot\frac{\Delta t}{N}=\frac{\Delta t\cdot\lambda\cdot V\cdot f_r}{4V_\pi\cdot n_g}。\tag{5}$$

本文所采用的 EOM(Thorlabs,EO-PM-NR-C3)的半波电压为 350 V,受制于实际条件,只能给 EOM 施加最高 200 V 的电压。当 EOM 的调制频率为 100 kHz 时,本振激光器的波长为 1557 nm,此时的最大测量范围为 351 μm,更新速率为 200 kHz。当更新速率降至 40 kHz 时,最大测量范围可扩大至 1.75 mm。

3　实验系统

整个测距系统分为光源模块、激光器同步模块、测距模块和数据采集与处理模块 4 个部分。光源模块采用两台重复频率约为 158 MHz 的 NPR 锁模激光器,分别作为信号激光器和本振激光器,其中:本振激光器的脉冲宽度为 140 fs,光谱宽度为 21 nm,中心波长为 1569 nm,平均功率为 20 mW,处于自由运转状态;信号激光器的脉冲宽度为 92 fs,光谱宽度为 51 nm,中心波长为 1557 nm,平均功率为 50 mW,通过调节压电陶瓷(PZT)使其重复频率与本振激光器锁定一致。两台激光器的输出光会分为两部分:一部分进入激光器同步模块,用来进行重复频率的锁定;

另一部分进入测距模块，用来产生测距信号，进行距离的解算。系统光路图如图 2 所示，其中图 2(a)为信号激光器的光谱图，图 2(b)为本振激光器的光谱图，图 2(c)为测距装置图。

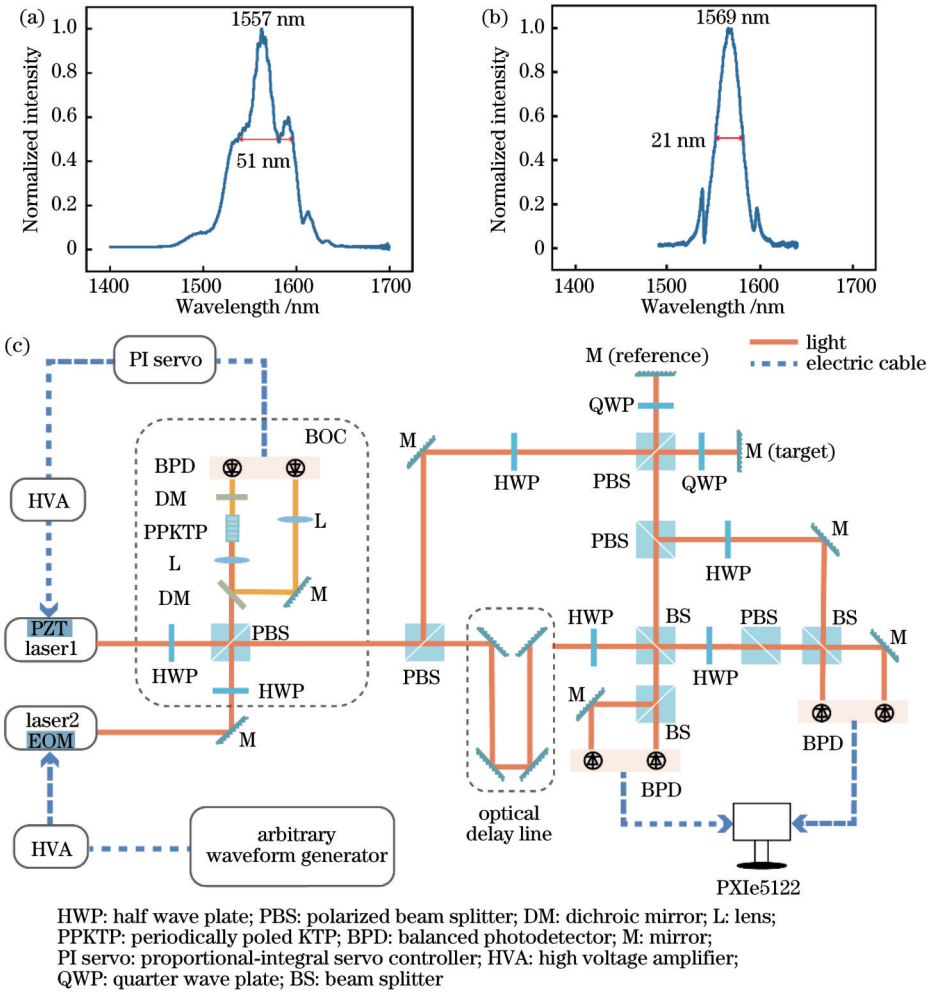

图 2　测距系统示意图。(a)信号激光器光谱；(b)本振激光器光谱；(c)实验装置

Fig. 2　Schematic diagram of distance measurement system. (a) Spectrum of signal laser; (b) spectrum of local laser; (c) experimental setup

为保证良好的锁定效果，激光器同步模块选择使用平衡光学互相关(BOC)系统。光源模块的两列输出光通过 HWP 调整用于重复频率锁定和距离测量的分光比后，利用 BOC 系统中的 PBS 进行合束，并将合束后的光分成两个部分。用于锁定重复频率的合束光通过透射 1550 nm 基频光、反射 775 nm 倍频光的 DM，经 L 聚焦后打入 PPKTP 晶体中，产生的倍频光通过反射 1550 nm 基频光、透射 775 nm 倍频光的 DM 后进入 BPD 的一个光电二极管中，而没有经过倍频的基频光在被 DM 反射后将再次经过 PPKTP 晶体，产生倍频光后经过第一个 DM 和 M 的反射后打入 BPD 的另一个光电二极管中。二者经过 BPD 作差后将误差信号输送到伺服控制器(New Focus，LB1005)中，得到控制 PZT 的实时电压，经过高压放大器放大后输送给信号激光器中的 PZT，形成锁相环路，从而进行重复频率的锁定，在锁定时，两列脉冲呈对准状态。

通过任意波形发生器产生一个振幅为 V、频率为 f_m、占空比为 0.5 的方波信号，此时的峰-峰值振幅为 $V_{pp}=2\cdot V$，经过 20 倍的高压放大器(Thorlabs，HVA200)放大后施加给 EOM，可通过调节振幅和频率的大小来控制采样脉冲在信号脉冲两侧往返走离的长度和干涉信号的更新速率。

用于产生测距信号的合束光的偏振态在经过 BOC 中的 PBS 后相互垂直。因此，在 BOC 系统后加入一个 PBS 便可将信号光与本振光进行分离，其中将反射光命名为信号光，透射光命名为本振光。解算距离值需要利用 PBS 将信号光分为参考光和目标光两个部分，在该 PBS 前加入了一个 HWP，用于调节参考光与目标光的分光比。信号光经过 PBS 后，透射光射入目标臂，反射光射入参考臂，经过参考镜与目标镜的反射后会得到两列具有一定时间延迟的偏振态相互垂直的回波脉冲序列。在参考臂与目标臂的光路中都加入一个 QWP，将垂直偏振态的参考光和水平偏振的目标光分别变为水平偏振态和垂直偏振态，从而使二者

在返回PBS的时候不会再次回到原来的信号光路中。

将参考回波脉冲与目标回波脉冲分开探测可避免测量死区的产生，故需将合束后的参考回波脉冲与目标回波脉冲再次利用PBS进行分离。为了使经过迈克耳孙干涉光路的信号光与本振光的脉冲序列能够再次对准，令本振光提前经过光学延迟线后再与参考回波脉冲和目标回波脉冲分别进行合束，产生干涉信号。由于平衡探测器可以抑制共模噪声，故在将合束后的光各自利用BS分束后用两个平衡探测器进行探测。利用采样率为100 MHz的数字化仪（National Instruments，PXIe5122）对干涉信号进行信号采集，利用希尔伯特变换提取包络得到峰值位置后，进行距离解算。为保证在实验过程中可以进行不同位置的距离测量，将参考臂和测量臂上的反射镜都固定在了位移台上。

4　实验结果

为了验证系统的重复性，利用信号发生器产生一个峰-峰值电压为20V_{pp}、频率为100 kHz、占空比为0.5的方波调制，经过20倍的高压放大器放大后，电压变成±200 V，交替施加到EOM上，此时的扫描范围可以通过式(3)计算，得到结果为351 μm。在此条件下，对41 μm的固定位置进行了更新速率为200 kHz的10000次重复性测量，此时的标准差为938 nm。为了提升精度，进行了100个点的滑动平均，之后标准差降至100 nm。测量结果如图3所示，由此可见此套系统具有良好的重复性。

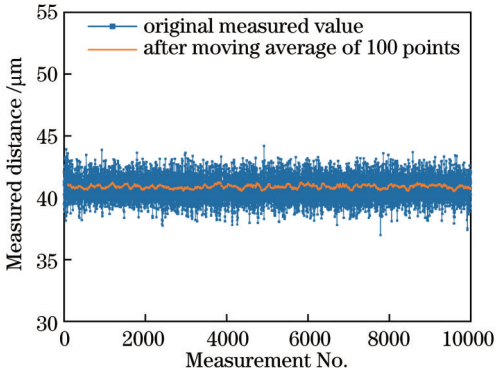

图3　41 μm静止距离的测量结果

Fig. 3　Measurement results of 41 μm static distance

为了证明此套系统具有良好的稳定性，同样产生±200 V调制电压交替施加到EOM上，利用该双飞秒激光距离测量系统对41 μm的固定距离进行了测量，图4给出了积分时间由0.005 ms连续变化至20.5 ms时的Allan方差。单次测量最快更新速率为200 kHz，由给EOM所加的调制频率决定，测量精度为1.14 μm。当平均时间为10.25 ms时，测量精度为27.3 nm，对应于2050次单次测量平均后得到的结果。当平均时间达到20.5 ms时，测量精度可以提高至16.7 nm，对应于4100次单次测量平均后得到的结果。由于实验室采集仪器的内存有限，故未能进行更长时间的结果测量。

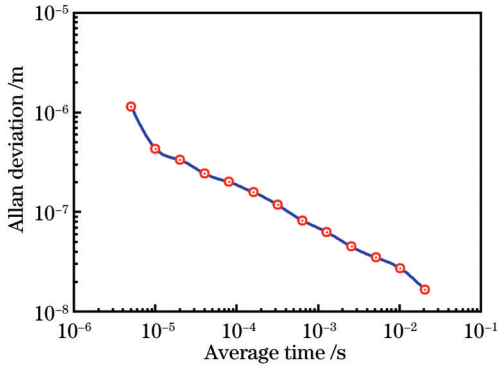

图4　41 μm绝对距离测量艾伦方差

Fig. 4　Allan deviation of 41 μm absolute distance measurement

为了验证此套系统的再现性，保证其他条件不变，给EOM施加了调制频率为100 kHz、具有不同峰-峰值调制电压的方波调制，对41 μm的固定位置进行了重复测量，将调制电压的改变范围设定为7V_{pp}～20V_{pp}，以V_{pp}为步长进行了14次测量，此时的测量范围为123～351 μm。对每次测量结果均进行2050次平均，测量结果如图5所示，测量标准差为417.2 nm。由此可见，虽然改变调制电压会带来测量范围的变化，但是同一位置的测量结果具有良好的再现性。

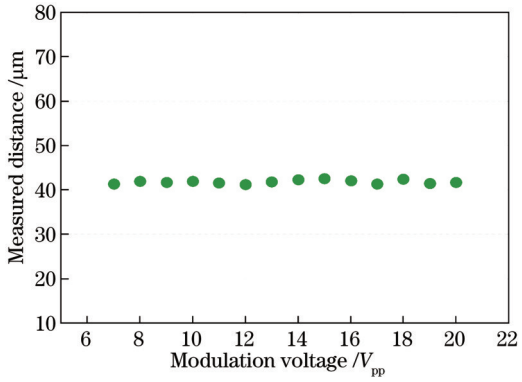

图5　不同调制电压时的距离测量结果

Fig. 5　Distance measurement results at different modulation voltages

为了验证此套测距系统测量结果的准确性，将固定峰-峰值为±200 V的调制电压交替施加到EOM上，将目标镜放置在20 μm处，以10 μm为步长进行移动，移动至90 μm处，共移动70 μm，每次测量结果均进行2050次平均。对比测量结果如图6所示，系统测量精度在百纳米级，残差分布在±528 nm以内，与真实距离拟合效果良好。

利用此套系统对硅基微机械结构中宽度为30 μm

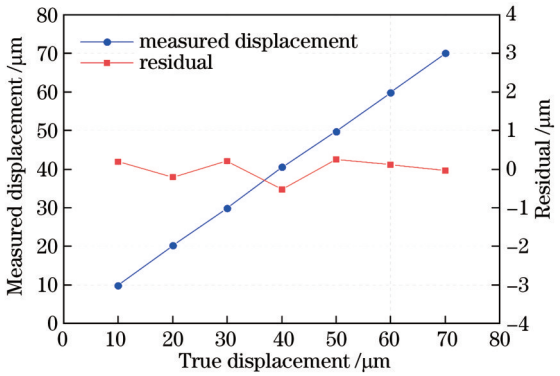

图 6　测量值与真实值的比较

Fig. 6　Comparison between measured values and real values

的凹槽进行了深度分析，待测样品如图 7(b)所示，将该样品固定在三维调整架上，替换了原本的目标反射镜，并在该待测样品前加入了一个焦距为 11 mm 的聚焦透镜(Thorlabs，C220TME-C)。由于光斑的聚焦位置需要能够进行前后调整，故将该聚焦透镜固定在了位移台上。由于凹槽深度未知，为了能够得到清晰且完整的干涉信号，故对 EOM 施加峰-峰值为±200 V、调制频率为 50 kHz 的交替电压，调制频率的降低使可测范围扩大为 702 μm。以 30 μm 为步长，对该凹槽进行了 10 个位置的深度测量。每次测量时间为 20.5 ms，对应于 2050 次平均后的结果，测量结果如图 7(a)所示。经测量，凹槽的平均深度约为 67.6 μm，标准差为 1.19 μm。

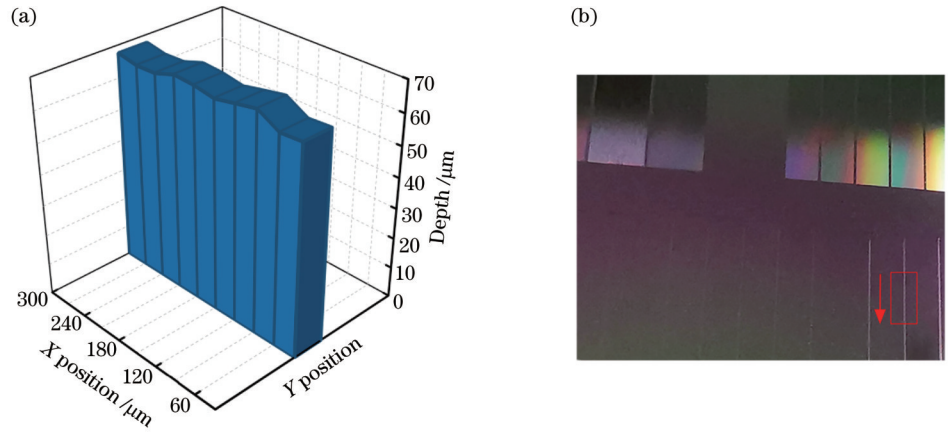

图 7　凹槽深度分析。(a)凹槽深度测量结果；(b)微机械器件

Fig. 7　Groove depth analysis. (a) Measurement result of groove depth; (b) micromechanical device

5　结　　论

提出了一种基于电控光学采样的双飞秒激光绝对距离测量系统。选择了两台重复频率皆约为 158 MHz 的 NPR 锁模激光器，通过激光器同步模块进行了重复频率的锁定，在经过空间延迟线对准后，通过给本振激光器中的电光调制器施加方波调制来使采样脉冲在信号脉冲的两侧来回走离。只对有效信号部分进行往返扫描克服了传统异步光学采样方法的更新速率受限于重复频率差和只能对整个扫描范围进行无差别采样的问题，与 Shi 等[25]工作相比，可测量范围得到扩大的同时，更新速率也到了进一步提升。在实验中，更新速率最高可达 200 kHz，测量 41 μm 绝对距离时，平均时间为 20.5 ms 的情况下测量精度可以达到 16.7 nm。在更新速率为 100 kHz 时，最大可测范围可达 702 μm，理论上将更新速率降到 40 kHz 时，最大可测量范围可扩大至 1.75 mm，满足大部分微机械结构、半导体器件等微纳器件中的深沟槽检测需求。通过实验证明了该系统具有良好的重复性、再现性、稳定性和准确性。同时，基于此套系统对微机械结构中的凹槽进行了深度分析。可以发现，基于电控光学采样的双飞秒激光系统在微距离测量中有着广泛的应用，在三维形貌扫描等领域中也有着良好的应用前景，如对器件的表面进行痕迹检测、对平面进行平整度分析等。

由于受到 EOM 的重复频率改变量和高压放大器放大倍数的限制，系统的最大可测范围还停留在毫米量级，通过更换重复频率改变量更大的 EOM 或者放大倍数更大的高压放大器，可以进一步扩大系统的测量范围和提高系统的更新速率。

参　考　文　献

[1] Newbury N R, Washburn B R. Theory of the frequency comb output from a femtosecond fiber laser[J]. IEEE Journal of Quantum Electronics, 2005, 41(11): 1388-1402.

[2] Fork R L, Greene B I, Shank C V. Generation of optical pulses shorter than 0.1 psec by colliding pulse mode locking[J]. Applied Physics Letters, 1981, 38(9): 671-672.

[3] 吴翰钟，曹士英，张福民，等. 光学频率梳基于光谱干涉实现绝对距离测量[J]. 物理学报，2015，64(2)：020601.
Wu H Z, Cao S Y, Zhang F M, et al. Spectral interferometry based absolute distance measurement using frequency comb[J]. Acta Physica Sinica, 2015, 64(2): 020601.

[4] Xu X Y, Zhao H H, Zhang Z Q, et al. Precise underwater distance measurement using laser frequency comb[J]. Metrologia, 2021, 58(1): 015009.

[5] 王一霖，杨凌辉，林嘉睿，等. 基于飞秒光学频率梳相关探测

的绝对测距[J]. 光学学报, 2019, 39(1): 0112003.
Wang Y L, Yang L H, Lin J R, et al. Absolute distance measurement based on coherent detection by femtosecond optical frequency comb[J]. Acta Optica Sinica, 2019, 39(1): 0112003.
[6] Bak S, Kim G H, Jang H, et al. Optical Vernier sampling using a dual-comb-swept laser to solve distance aliasing[J]. Photonics Research, 2021, 9(5): 657-667.
[7] Gambetta A, Gatti D, Castrillo A, et al. Comb-assisted spectroscopy of CO_2 absorption profiles in the near- and mid-infrared regions[J]. Applied Physics B, 2012, 109(3): 385-390.
[8] 杨昌喜, 赵康俊, 曹博, 等. 单腔双光梳锁模光纤激光器及其应用研究进展[J]. 中国激光, 2021, 48(15): 1501001.
Yang C X, Zhao K J, Cao B, et al. Recent progress of single-cavity dual-comb mode-locked fiber lasers and their applications [J]. Chinese Journal of Lasers, 2021, 48(15): 1501001.
[9] 路桥, 时雷, 毛庆和. 双光梳光谱技术研究进展[J]. 中国激光, 2018, 45(4): 0400001.
Lu Q, Shi L, Mao Q H. Research advances in dual-comb spectroscopy[J]. Chinese Journal of Lasers, 2018, 45(4): 0400001.
[10] Han S, Kim Y J, Kim S W. Parallel determination of absolute distances to multiple targets by time-of-flight measurement using femtosecond light pulses[J]. Optics Express, 2015, 23(20): 25874-25882.
[11] Kim W, Jang J, Han S, et al. Absolute laser ranging by time-of-flight measurement of ultrashort light pulses[J]. Journal of the Optical Society of America A, 2020, 37(9): B27-B35.
[12] Yang H Z, Zhao C M, Zhang H Y, et al. A novel hybrid TOF/phase-shift method for absolute distance measurement using a falling-edge RF-modulated pulsed laser[J]. Optics & Laser Technology, 2019, 114: 60-65.
[13] Dorrer C, Kilper D C, Stuart H R, et al. Linear optical sampling [J]. IEEE Photonics Technology Letters, 2003, 15(12): 1746-1748.
[14] Coddington I, Swann W C, Nenadovic L, et al. Rapid and precise absolute distance measurements at long range[J]. Nature Photonics, 2009, 3(6): 351-356.
[15] 吴冠豪, 周思宇, 杨越棠, 等. 双光梳测距及其应用[J]. 中国激光, 2021, 48(15): 1504002.
Wu G H, Zhou S Y, Yang Y T, et al. Dual-comb ranging and its applications[J]. Chinese Journal of Lasers, 2021, 48(15): 1504002.
[16] Zhu Z B, Wu G H. Dual-comb ranging[J]. Engineering, 2018, 4 (6): 772-778.
[17] Liu Y, Xia W Z, He M Z, et al. Experimental realization and characterization of a two-color dual-comb system for practical large-scale absolute distance measurements[J]. Optics and Lasers in Engineering, 2022, 151: 106900.
[18] Han J B, Li S Y, Wu T F, et al. Time-of-flight absolute distance measurement with dual-comb[J]. Proceedings of SPIE, 2018, 10697: 106972R.
[19] Hu D T, Wu Z L, Cao H, et al. Dual-comb absolute distance measurement of non-cooperative targets with a single free-running mode-locked fiber laser[J]. Optics Communications, 2021, 482: 126566.
[20] Zhang H Y, Wei H Y, Wu X J, et al. Absolute distance measurement by dual-comb nonlinear asynchronous optical sampling[J]. Optics Express, 2014, 22(6): 6597-6604.
[21] Kim Y, Yee D S. High-speed terahertz time-domain spectroscopy based on electronically controlled optical sampling [J]. Optics Letters, 2010, 35(22): 3715-3717.
[22] Dietz R J B, Vieweg N, Puppe T, et al. All fiber-coupled THz-TDS system with kHz measurement rate based on electronically controlled optical sampling[J]. Optics Letters, 2014, 39(22): 6482-6485.
[23] Kray S, Spöler F, Hellerer T, et al. Electronically controlled coherent linear optical sampling for optical coherence tomography [J]. Optics Express, 2010, 18(10): 9976-9990.
[24] Kameyama R, Takizawa S, Hiramatsu K, et al. Dual-comb coherent Raman spectroscopy with near 100% duty cycle[J]. ACS Photonics, 2021, 8(4): 975-981.
[25] Shi Y Y, Hu D T, Xue R, et al. High speed time-of-flight displacement measurement based on dual-comb electronically controlled optical sampling[J]. Optics Express, 2022, 30(5): 8391-8398.
[26] 马雪莲, 刘璐, 张志刚, 等. 平衡式光学互相关方案测量光脉冲传输抖动的理论和实验研究[J]. 光学学报, 2010, 30(1): 59-64.
Ma X L, Liu L, Zhang Z G, et al. Theoretical and experimental study on timing jitter measurement for transmitted pulse using balanced optical cross correlation scheme[J]. Acta Optica Sinica, 2010, 30(1): 59-64.

Femtosecond Laser Distance Measurement Based on Electronically Controlled Optical Sampling

Xue Rui, Wu Ziling, Dong Jiaqi, Hu Minglie, Song Youjian*

Key Laboratory of Optoelectronic Information Technology Science, Ministry of Education, School of Precision Instrument and Opto-Electronics Engineering, Tianjin University, Tianjin 300072, *China*

Abstract

Objective Time-of-flight distance measurement based on a dual-comb approach is widely applied in the fields of laser radar, topography scanning, and vibration measurement by using two femtosecond lasers with a small repetition frequency difference for asynchronous optical sampling (ASOPS). In this manner, the high temporal resolution, comb-shaped spectrum, and ultra-low noise performance of femtosecond lasers can be fully utilized. However, the update rate of a dual-comb ranging system based on ASOPS is limited to a few kilohertz (determined by the repetition frequency difference) so as to avoid insufficient optical sampling. Given the extremely small duty cycle determined by the ratio of the femtosecond

pulse width to the millisecond sampling period, most of the sampling time during a full sampling cycle is wasted in the process of pulse walk-off. To solve this problem, an electro-optical modulator (EOM) is added to the ASOPS system to modulate the repetition frequency periodically in this work. The so-called electronically controlled optical sampling (ECOPS) approach breaks the update rate limitation in the ASOPS system and can increase the update rate to hundreds of kilohertz, further enriching the application fields of dual-comb distance measurement technology.

Methods ECOPS uses two lasers with tightly phase-locked repetition frequency (f_r) as the light source. One is called a local laser with an EOM inserted in the cavity, and the other is called a signal laser. The EOM in the cavity is used to modulate the repetition frequency of the local laser. As a square wave is imposed on the EOM, the repetition frequency is switched between $f_r-\Delta f_r$ and $f_r+\Delta f_r$, and the modulation period is determined by the square wave modulation frequency f_m. Therefore, the repetition frequency difference between the two lasers switches between $-\Delta f_r$ and Δf_r at the modulation frequency f_m. Different from ASOPS with only a fixed Δf_r, the rapid switching of $\pm\Delta f_r$ effectively drives the output pulse of the local laser to scan back and forth on both sides of the output pulse of the signal laser, resulting in a controlled, bounded optical sampling and avoiding the unwanted pulse walk-off. The update rate is determined by the modulation frequency f_m, which breaks the limitation of the ASOPS-based measurement system where the update rate is determined by the repetition frequency difference Δf_r. In the experiment, a pair of nonlinear polarization rotation (NPR) mode-locked fiber lasers with a repetition frequency of ~158 MHz are selected as the signal laser and the local laser. In the local laser, the pulse duration is 140 fs, the spectral width is 21 nm, the central wavelength is 1569 nm and the average power is 20 mW. As for the signal laser, the pulse duration is 92 fs, the spectral width is 51 nm, the central wavelength is 1557 nm and the average power is 50 mW. Part of the output of the two lasers is combined and directed to a balanced optical cross-correlator (BOC), which detects the relative timing error between the two lasers with sub-femtosecond resolution. The error signal is fed back to the end mirror mounted on a fast piezo-actuator such that the repetition frequencies of the two fiber lasers are tightly phase-locked, and the residual timing jitter is lower than a few femtoseconds. After the phase locking of repetition frequencies is established, the main parts of the laser output are directed to the distance measurement module. A mechanical delay line is used to adjust the optical path from the output of one laser so as to make sure that the pulses from the two lasers overlap in time. As square wave modulation is applied to the EOM, the signal pulses naturally scan back and forth on both sides of the local pulses, which enables ECOPS-based distance measurement.

Results and Discussions A $\pm$200 V, 100 kHz square wave with a duty cycle of 0.5 is used in the experiments. The maximum update rate of a single measurement is up to 200 kHz, and the detectable range is 351 μm. The measurement accuracy reaches 16.7 nm after 4100 times of averaging (Fig. 4), and the system has been proven to have good accuracy and stability. At an update rate of 200 kHz and a static distance of 41 μm, the standard deviation of 10000 consecutive measurements is 938 nm. The standard deviation can be reduced to 100 nm after moving average of 100 points (Fig. 3). Therefore, the system has been proven to have good repeatability. In addition, multiple measurements at the same location at different Δf_r show a standard deviation of 417.2 nm after 2050 times of averaging (Fig. 5), which reflects that the system has good reproducibility. Then, the target object is moved with each step of 10 μm, and after 2050 times of averaging, the measured values are compared with the true values. The measurement accuracy of the system is within a few hundred nanometers, and the residual is within $\pm$528 nm (Fig. 6), which indicates that the system has good accuracy. To prove the capability of the system to detect surface traces, a silicon-based micromechanical device [Fig. 7(b)] is measured. In the measurement, a $\pm$200 V, 50 kHz square wave modulation with a duty cycle of 0.5 is applied to the EOM. The update rate is 100 kHz at this time, and the detectable range is 702 μm. Ten positions are measured with a lateral spacing of 30 μm between every two positions. The original ranging data of each position is averaged by 2050 times, and then the trench depth is calculated to be about 67.6 μm [Fig. 7(a)]. The proposed absolute distance measurement system has high accuracy and update rate, and can be applied in the 3D surface profile measurement of micromechanical structures. This system is also suitable for high-frequency mechanical vibration monitoring.

Conclusions This paper proposes a dual-comb absolute distance measurement system based on ECOPS and selects two NPR mode-locked lasers with a repetition frequency of ~158 MHz. In the experiment, their repetition frequencies are locked by the synchronization module. After the two femtosecond pulse trains are aligned through the spatial delay line, the sampling pulse is moved back and forth on both sides of the signal pulse by adding a square wave to the EOM in the local laser, which overcomes the problem in the ASOPS approach where the update rate is limited by the repetition frequency difference. The update rate of the experimental setup can be up to 200 kHz, and the measurement accuracy can reach 16.7 nm with an average time of 20.5 ms in the measurement of an absolute distance of 41 μm. In theory, when the update rate is reduced to 40 kHz, the detectable range can reach 1.75 mm, which meets the detection requirements of trenches in most micromechanical structures, semiconductor devices, and other micro-nano devices. The experiments show that the system has good repeatability, reproducibility, stability, and accuracy. The trench depth in a

micromechanical structure is measured with the designed system. The dual-comb system based on ECOPS can be widely used in micro-distance measurement, and also has potential application prospects in the fields of 3D topography scanning, such as surface profilometry and flatness analysis.

Key words measurement; femtosecond pulse; electronically controlled optical sampling; flight time; absolute distance measurement